

A condensing approach for linear-quadratic optimization with geometric constraints

Alberto De Marchi*

Abstract

Optimization problems with convex quadratic cost and polyhedral constraints are ubiquitous in signal processing, automatic control and decision-making. We consider here an enlarged problem class that allows to encode logical conditions and cardinality constraints, among others. In particular, we cover also situations where parts of the constraints are nonconvex and possibly complicated, but it is practical to compute projections onto this nonconvex set. Our approach combines the augmented Lagrangian framework with a solver-agnostic structure-exploiting subproblem reformulation. While convergence guarantees follow from the former, the proposed condensing technique leads to significant improvements in computational performance.

Keywords. Linear-quadratic optimization, Augmented Lagrangian, Geometric constraints, Projection oracle

Contents

1	Introduction	2
2	Optimality and Stationarity	3
3	Augmented Lagrangian Method	4
3.1	Safeguarded augmented Lagrangian scheme	4
3.2	Convergence and infeasibility detection	4
3.3	Inner solver: projected gradient	5
4	Condensing: How and Why	6
4.1	Evaluating the marginal function	6
4.2	Lower-level equality constraints	7
5	Numerical Results	7
5.1	Initial value problem	8
5.2	Obstacle problem	9
5.3	AFTI-16 tracking control	9
6	Conclusions	11
References		11
A	Additional Material	13
A.1	Globally Lipschitz gradient	13
A.2	Structured linear system	13
A.3	AFTI-16 model	13
A.4	Scalability outcomes	14

*University of the Bundeswehr Munich, Department of Aerospace Engineering, Institute of Applied Mathematics and Scientific Computing, 85577 Neubiberg/Munich, Germany, EMAIL alberto.demarchi@unibw.de, ORCID [0000-0002-3545-6898](https://orcid.org/0000-0002-3545-6898).

1 Introduction

This work presents a numerical approach for addressing finite-dimensional optimization problems of the form

$$\begin{aligned} & \underset{x}{\text{minimize}} \quad f(x) := \frac{1}{2} \langle x, Qx \rangle + \langle q, x \rangle \\ & \text{subject to} \quad Ax \in \mathcal{C} \end{aligned} \tag{1}$$

where $x \in \mathbb{R}^n$ are the decision variables, $f: \mathbb{R}^n \rightarrow \mathbb{R}$ is a convex quadratic function, $A \in \mathbb{R}^{m \times n}$ is a matrix, and $\mathcal{C} \subset \mathbb{R}^m$ a nonempty closed set. Model (1) covers classical convex quadratic programs (QP) with linear equality and inequality constraints, but it includes much more, as it allows \mathcal{C} be nonconvex. In view of control applications, the class (1) includes classical instances of discrete-time optimal control problems which arise, for instance, by time discretization of linear-quadratic problems of the form

$$\begin{aligned} & \underset{x(\cdot), y(\cdot), u(\cdot)}{\text{minimize}} \quad \int_0^T \|y(t) - y_{\text{ref}}(t)\|^2 + \|u(t) - u_{\text{ref}}(t)\|^2 \\ & \text{subject to} \quad \dot{x}(t) = F(x(t), u(t)), \quad y(t) = G(x(t)) \\ & \quad x(t) \in X, \quad u(t) \in U, \quad x(0) = x_{\text{init}}. \end{aligned}$$

When the dynamics F and the observation model G are linear, one recovers an instance of (1) upon time discretization. Our interest in addressing (1) for general, not necessarily convex, \mathcal{C} lies in the possibility to specify complicated constraints in a natural form.

In practice, for (1) we additionally assume only that \mathcal{C} admits an easy-to-evaluate projection operator. Examples of projection-friendly sets are those commonly arising in models known as mathematical programs with equilibrium constraints (MPEC); they often result from the union of finitely many simple sets (disjunctive form). Notable instances are complementarity (CC), switching (SC), vanishing (VC), and either-or constraints (EOC), defined respectively by

$$\begin{aligned} \text{CC:} \quad & \{(a, b) \in \mathbb{R}_+^2 \mid ab = 0\}, \\ \text{SC:} \quad & \{(a, b) \in \mathbb{R}^2 \mid ab = 0\}, \\ \text{VC:} \quad & \{(a, b) \in \mathbb{R}^2 \mid a \geq 0 \wedge ab \geq 0\}, \\ \text{EOC:} \quad & \{(a, b) \in \mathbb{R}^2 \mid a \leq 0 \vee b \geq 0\}. \end{aligned}$$

Among others, complementarity sets appear when modelling nonsmooth dynamics [16] and contact mechanics [12], while vanishing constraints play a role in mixed-integer optimal control [14, 15]. Nonconvex sets \mathcal{C} naturally appear when encoding logical constraints [3], as EOC is equivalent to $a > 0 \implies b \geq 0$. Even binary sets intersected with linear constraints can be deemed projection-friendly, since the associated projection operator boils down to solving a binary linear program, and they can be adopted to specify combinatorial constraints and sparsity-promoting regularization costs [13].

Unfortunately, the numerical treatment of optimization problems with disjunctive constraints is often ineffective with standard nonlinear programming techniques, since constraint qualifications are likely to fail at interesting feasible points. Regularization [7], relaxation [9] and penalty [6] schemes have been widely investigated and adopted to overcome this difficulty. However, their implementation remains limited to specific constraints, as the associated tools (such as regularization terms and penalty functions) must be tailored to the constraint set \mathcal{C} . Conversely, Jia et al. [8] study a generic approach to treat possibly complicated constraints, accessing \mathcal{C} only via its projection operator. In the generality of their (nonlinear nonconvex) setting, however, it is difficult to take advantage of other structures that the problem may have.

Contribution In this paper we build upon the generic approach of [8] to treat the geometric constraints, inheriting its rigorous theoretical guarantees, while leveraging the linear-quadratic structure in (1) for computational efficiency. The proposed numerical scheme poses minimal assumptions (mere convexity of f), is robust to redundant constraints, and handles the constraint set \mathcal{C} only through its projection oracle. The advantages (faster convergence, scalability and greater flexibility) are showcased across a range of control tasks. Further speed-up is demonstrated when exploiting also “safe” equality constraints, e.g., those arising from dynamics.

Outline The notion of solution is discussed in Section 2 before describing the augmented Lagrangian framework in Section 3. The condensing approach and related procedure are detailed in Section 4. Numerical results and comparisons are reported in Section 5.

Notation Given a set $S \subseteq \mathbb{R}^m$, its INDICATOR is defined by $\mathcal{I}_S(v) = 0$ if $v \in S$, and $\mathcal{I}_S(v) = \infty$ otherwise. The associated PROJECTION $\text{proj}_S: \mathbb{R}^m \rightrightarrows \mathbb{R}^m$ is defined by $\text{proj}_S(v) := \arg \min_{z \in S} \|z - v\|$, while $\text{dist}_S(v) := \inf_{z \in S} \|z - v\|$ indicates the DISTANCE of v from S . The identity matrix \mathbb{I} has suitable size, clear from the context.

2 Optimality and Stationarity

Problem (1) can be rewritten in the equivalent form

$$\underset{x, z}{\text{minimize}} \quad f(x) + \mathcal{I}_{\mathcal{C}}(z) \quad \text{subject to} \quad Ax - z = 0 \quad (2)$$

by introducing the auxiliary variable $z \in \mathbb{R}^m$. Then, the LAGRANGIAN FUNCTION for (2) reads

$$\mathcal{L}(x, z, y) := f(x) + \mathcal{I}_{\mathcal{C}}(z) + \langle y, Ax - z \rangle \quad (3)$$

where $y \in \mathbb{R}^m$ denotes the Lagrange multiplier associated to the equality constraints. By differentiation one obtains the following stationarity conditions, necessary for first-order optimality (under suitable constraint qualifications):

$$0 = \nabla_x \mathcal{L}(x, z, y) = \nabla f(x) + A^\top y, \quad (4a)$$

$$0 \in \partial_z \mathcal{L}(x, z, y) = \mathcal{N}_{\mathcal{C}}^{\text{lim}}(z) - y, \quad (4b)$$

$$0 = \nabla_y \mathcal{L}(x, z, y) = Ax - z, \quad (4c)$$

where ∂ and $\mathcal{N}_{\mathcal{C}}^{\text{lim}}$ denote the limiting subdifferential and the limiting normal cone to \mathcal{C} , respectively, as in [8]. The ‘‘limiting’’ character appears as \mathcal{C} is potentially nonconvex. Formally eliminating the auxiliary z , the stationarity conditions for the original problem (1) read

$$0 = \nabla f(x) + A^\top y, \quad y \in \mathcal{N}_{\mathcal{C}}^{\text{lim}}(Ax), \quad (5)$$

where the inclusion encodes both feasibility of x , as it implies $Ax \in \mathcal{C}$, and complementarity of y with the constraint.¹ A point $x \in \mathbb{R}^n$ is called a FRITZ-JOHN (FJ) point for (1) if there exists $(\mu, y) \in \mathbb{R} \times \mathbb{R}^m$ with $(\mu, y) \neq 0$ such that

$$0 = \mu \nabla f(x) + A^\top y, \quad y \in \mathcal{N}_{\mathcal{C}}^{\text{lim}}(Ax). \quad (6)$$

A FJ point is a KARUSH-KUHN-TUCKER (KKT) point whenever $\mu \neq 0$. In that case, y/μ is the associated vector of Lagrange multipliers. A FJ point for which $\mu = 0$ is called a SINGULAR STATIONARY point: a feasible point at which constraint qualifications fail (e.g., LICQ does not hold). A point $x \in \mathbb{R}^n$ is called an INFEASIBLE STATIONARY point of problem (1) if $Ax \notin \mathcal{C}$ and $A^\top [Ax - \text{proj}_{\mathcal{C}}(Ax)] = 0$: an infeasible point for (1) that is a stationary point for the feasibility problem $\underset{x}{\text{minimize}} \text{dist}_{\mathcal{C}}^2(Ax)$.

For implementing an iterative numerical procedure, a termination condition can be based on an approximate notion of optimality. Given some tolerances $\epsilon_d, \epsilon_p > 0$, a point $x \in \mathbb{R}^n$ is called (ϵ_d, ϵ_p) -STATIONARY (in the FJ sense) if there exists $(\mu, y, z) \in \mathbb{R} \times \mathbb{R}^m \times \mathcal{C}$ with $(\mu, y) \neq 0$ such that the conditions

$$\|\mu \nabla f(x) + A^\top y\| \leq \epsilon_d \quad (7a)$$

$$\text{dist}(y, \mathcal{N}_{\mathcal{C}}^{\text{lim}}(z)) \leq \epsilon_d \quad (7b)$$

$$\|Ax - z\|_\infty \leq \epsilon_p \quad (7c)$$

are satisfied, see (4) and (6). Tolerances ϵ_d and ϵ_p reflect the relaxation on dual and primal residuals, respectively.

¹Observe that, for any $\alpha > 0$, the condition $Ax \in \text{proj}_{\mathcal{C}}(Ax + \alpha y)$ implies $y \in \mathcal{N}_{\mathcal{C}}^{\text{lim}}(Ax)$. In contrast, due to nonconvexity of \mathcal{C} , the converse implication $y \in \mathcal{N}_{\mathcal{C}}^{\text{lim}}(Ax) \implies Ax \in \text{proj}_{\mathcal{C}}(Ax + \alpha y)$ is valid only for sufficiently small $\alpha > 0$. For convex \mathcal{C} , they are equivalent for all $\alpha > 0$.

3 Augmented Lagrangian Method

The auxiliary variable $z \in \mathbb{R}^m$ has been introduced in (2) to derive the stationarity conditions for (1) and to define a suitable termination criterion based on approximate optimality. However, the expression of problem (1) in the splitting form (2) is also closer to the numerical procedure described below, as it allows us to favorably decouple the linear operator A from the set \mathcal{C} . We will relax and penalize violation of the linear constraint $Ax = z$, following the augmented Lagrangian (AL) framework [8, 2]. This entails solving a sequence of subproblems, at least inexactly and up to stationarity (in contrast to global optimality), and then updating some parameters based on the progress thus obtained. A key role is played by the augmented Lagrangian function for (2), here defined for all $x \in \mathbb{R}^n$, $z \in \mathcal{C}$ by

$$\mathcal{L}_\sigma(x, z, \hat{x}, \hat{y}) := \mu f(x) + \frac{\rho}{2} \|x - \hat{x}\|^2 + \langle \hat{y}, Ax - z \rangle + \frac{1}{2} \|Ax - z\|^2, \quad (8)$$

for a given primal-dual estimate $(\hat{x}, \hat{y}) \in \mathbb{R}^n \times \mathbb{R}^m$ and a pair of positive penalty parameters $\sigma := (\rho, \mu)$. Note that, for reasons of numerical stability, we prefer to scale down the cost function f instead of increasing the quadratic constraint penalization, following [1], while also adding a proximal term for Tikhonov-like primal regularization.

3.1 Safeguarded augmented Lagrangian scheme

The AL approach requires solving subproblems of the form

$$\underset{x, z}{\text{minimize}} \quad \mathcal{L}_{\sigma_k}(x, z, \hat{x}_k, \hat{y}_k) \quad \text{subject to } z \in \mathcal{C}, \quad (\text{AL}_k)$$

up to approximate stationarity, to obtain the next primal estimate (x_k, z_k) . The overall scheme is outlined in [Algorithm 3.1](#), where it is clear that the minimization of (AL_k) is the most computationally demanding task. To alleviate this effort, warm-starting [Step 1](#) from the current estimate (\hat{x}_k, \hat{z}_k) is a common practice. After the primal update, [Step 1](#) generates a dual estimate $y_k \leftarrow \hat{y}_k + Ax_k - z_k$ by matching the subproblem's stationarity conditions with the KKT conditions for (2). Note that, at [Step 1](#), we adopt the safeguarding scheme of [2, §4] to guarantee global convergence: the previous dual estimate is projected onto a compact (arbitrarily large) set $Y \subset \mathbb{R}^m$ to obtain \hat{y}^k . Then, [Step 1](#) tests if the current primal-dual point is (ϵ_d, ϵ_p) -stationary, returning when successful. Owing to the ε_k -stationarity conditions for (AL_k) and the dual update at [Step 1](#), every triplet (x_k, z_k, y_k) satisfies

$$\begin{aligned} \|\mu_k \nabla f(x_k) + A^\top y_k + \rho_k(x_k - \hat{x}_k)\| &\leq \varepsilon_k \\ \text{dist}(y_k, \mathcal{N}_{\mathcal{C}}^{\text{lim}}(z_k)) &\leq \varepsilon_k, \end{aligned}$$

meaning that it suffices to check the computable quantities E_k and V_k defined at [Step 1](#) to assert approximate optimality of x_k , in the sense of (7).

Finally, the penalty parameters and tolerance controlling the inner minimization are updated. If a sufficient reduction of the infeasibility measure V_k has been obtained, both penalty parameters are kept constant and the inner tolerance is decreased at [Step 1](#). Otherwise, the latter remains constant and the penalty parameters are reduced at [Step 1](#).

Before discussing how the subproblem at [Step 1](#) can be solved with off-the-shelf methods, let us review some convergence guarantees available for [Algorithm 3.1](#).

3.2 Convergence and infeasibility detection

An essential property of [Algorithm 3.1](#) is that subproblem (AL_k) is well-posed for every $\sigma_k > 0$, $\hat{x}_k \in \mathbb{R}^n$ and $\hat{y}_k \in \mathbb{R}^m$. This fact follows from the strict convexity of the augmented Lagrangian $\mathcal{L}_{\sigma_k}(\cdot, \cdot, \hat{x}_k, \hat{y}_k)$ and closedness of set \mathcal{C} . Then, classical convergence guarantees are directly inherited from [8, Thm 4.3], [1, Thm 4.1]. The main observation is that feasible limit points are automatically KKT points (under constraints qualifications; see the references for analogous results under weaker assumptions).

Algorithm 3.1: Safeguarded augmented Lagrangian scheme

Input: $x^0 \in \mathbb{R}^n$, $y^0 \in \mathbb{R}^m$, $z^0 \in \mathbb{R}^m$, $\epsilon_p, \epsilon_d > 0$
Data: $\kappa_V \in [0, 1)$, $\kappa_\varepsilon, \kappa_\mu \in (0, 1)$, $\kappa_\rho \in (0, 1]$, $\varepsilon_1, \mu_1, \rho_1 > 0$, $Y \subset \mathbb{R}^m$ compact

- 1 $V_0 \leftarrow \infty$
- 2 **for** $k = 1, 2, \dots$ **do**
- 3 $(\hat{x}_k, \hat{z}_k, \hat{y}_k) \leftarrow (x_{k-1}, z_{k-1}, \text{proj}_Y(y_{k-1}))$
- 4 $(x_k, z_k) \leftarrow \varepsilon_k$ -stationary point of (AL_k)
- 5 $y_k \leftarrow \hat{y}_k + Ax_k - z_k$
- 6 $E_k \leftarrow \max\{\|\mu_k \nabla f(x_k) + A^\top y_k\|, \varepsilon_k\}$
- 7 $V_k \leftarrow \|Ax_k - z_k\|_\infty$
- 8 **if** $E_k \leq \epsilon_d$ and $V_k \leq \epsilon_p$ **then return** (x_k, z_k, y_k)
- 9 **if** $V_k \leq \max\{\epsilon_p, \kappa_V V_{k-1}\}$ **then**
- 10 $\rho_{k+1}, \mu_{k+1} \leftarrow \rho_k, \mu_k$ and $\varepsilon_{k+1} \leftarrow \kappa_\varepsilon \max\{\epsilon_d, \varepsilon_k\}$
- 11 **else**
- 12 $\rho_{k+1}, \mu_{k+1} \leftarrow \kappa_\rho \rho_k, \kappa_\mu \mu_k$ and $\varepsilon_{k+1} \leftarrow \varepsilon_k$

Proposition 3.1. Suppose matrix A in (1) has full rank and the sequence $\{\varepsilon_k\}$ in Algorithm 3.1 satisfies $\varepsilon_k \rightarrow 0$. Then each feasible accumulation point (\bar{x}, \bar{z}) of a sequence $\{(x_k, z_k)\}$ generated by Algorithm 3.1 is a KKT point of (2). In particular, each feasible accumulation point \bar{x} of $\{x_k\}$ is a KKT point of (1).

Since the feasible set (1) is nonconvex, it may happen that a limit point is not feasible, but even in this case it contains some useful information: infeasible limit points are stationary for the constraint violation [8, Prop. 4.2], [2, Thm 6.3].

Proposition 3.2. Suppose the sequence $\{\varepsilon_k\}$ in Algorithm 3.1 is bounded. Then each accumulation point \bar{x} of a sequence $\{x_k\}$ generated by Algorithm 3.1 is a stationary point for the so-called feasibility problem

$$\underset{x}{\text{minimize}} \quad \text{dist}_C^2(Ax).$$

3.3 Inner solver: projected gradient

The subproblems (AL_k) arising at Step 1 of Algorithm 3.1 have the general form

$$\underset{w}{\text{minimize}} \quad \varphi(w) \quad \text{subject to } w \in W \tag{9}$$

with a continuously differentiable function $\varphi: \mathbb{W} \rightarrow \mathbb{R}$ and some nonempty, closed set $W \subset \mathbb{W}$ (with easy-to-evaluate projection operator), where \mathbb{W} is an arbitrary Euclidean space. One can use $w := (x, z)$, $W := \mathbb{R}^n \times C$, and function $\varphi := w \mapsto \mathcal{L}_{\sigma_k}(x, z, \hat{x}_k, \hat{y}_k)$ to recover (AL_k) .

The prototypical method for addressing (9) is known as *projected gradient*, for which neither φ nor W need to be convex [8, §3]. Iterates are constructed based on the update rule

$$w_{j+1} \leftarrow \text{proj}_W(w_j - \gamma_j \nabla \varphi(w_j)),$$

where $\gamma_j > 0$ is a suitable stepsize, typically obtained by backtracking linesearch to deliver sufficient decrease in the cost φ . The projection operation ensures that each iterate is feasible, namely $w_j \in W$ for all $j \in \mathbb{N}$. Projected, or semismooth, Newton-type methods can achieve fast convergence but are applicable only to simple sets W in practice (such as hyperboxes). In contrast, first-order schemes such as projected gradient are more flexible and can benefit from nonmonotone globalization mechanisms [4, 8] as well as (quasi-Newton) extrapolation techniques [5].

4 Condensing: How and Why

Although subproblem (AL_k) can be solved with off-the-shelf solvers without additional effort, its special structure is particularly favorable and should be exploited. Since [Step 1](#) has the highest computational cost in [Algorithm 3.1](#), the overall solver performance can improve significantly. We demonstrate how to take advantage of it, on top of warm-starting the inexact solves at [Step 1](#), before assessing its beneficial effects with numerical examples.

Our starting point here is the observation that, for fixed $z \in \mathcal{C}$, (AL_k) becomes an unconstrained problem in x with a strictly convex quadratic objective:

$$\underset{x}{\text{minimize}} \quad \mu f(x) + \frac{1}{2} \|Ax - z + \hat{y}\|^2 + \frac{\rho}{2} \|x - \hat{x}\|^2. \quad (10)$$

Therefore, for any given $z \in \mathcal{C}$ there is a unique optimal x to minimize $\mathcal{L}_{\sigma_k}(\cdot, z, \hat{x}_k, \hat{y}_k)$; we denote $\mathcal{X}_k: \mathcal{C} \rightarrow \mathbb{R}^n$ this single-valued mapping. How to efficiently evaluate \mathcal{X}_k will be the topic of [Section 4.1](#). With this in mind, we can also define the (marginal) function $\mathcal{M}_k: \mathcal{C} \rightarrow \mathbb{R}$ as

$$\begin{aligned} \mathcal{M}_k(z) &:= \underset{x}{\text{minimize}} \mathcal{L}_{\sigma_k}(x, z, \hat{x}_k, \hat{y}_k) \\ &= \mathcal{L}_{\sigma_k}(\mathcal{X}_k(z), z, \hat{x}_k, \hat{y}_k), \end{aligned} \quad (11)$$

which gives the equivalent, yet *condensed* AL subproblem

$$\underset{z}{\text{minimize}} \quad \mathcal{M}_k(z) \quad \text{subject to } z \in \mathcal{C}. \quad (\text{CAL}_k)$$

Inspired by the “implicit” approach in [\[17\]](#), the formal minimization over the original variable x leaves us with a subproblem in the auxiliary variable z only. Note that (CAL_k) is again of the form [\(9\)](#), and it is smaller in size than (AL_k) , as well as better conditioned [\[17, Thm 1\]](#).

Crucially in practice, \mathcal{M}_k is continuously differentiable and has, in fact, even globally Lipschitz continuous gradient; see [Section A.1](#). Moreover, its value and gradient are relatively cheap to compute, as we illustrate below. (CAL_k) is the *condensed* counterpart of (AL_k) and can be addressed with the same off-the-shelf tools. Therefore, one can easily replace [Step 1](#) of [Algorithm 3.1](#) with

- $z_k \leftarrow \varepsilon_k$ -stationary point of (CAL_k) ,
- $x_k \leftarrow \mathcal{X}_k(z_k)$.

4.1 Evaluating the marginal function

By construction, \mathcal{X}_k returns the unique minimizer x of $\mathcal{L}_{\sigma_k}(\cdot, z, \hat{x}_k, \hat{y}_k)$, given $z \in \mathcal{C}$. Owing to convexity, this corresponds to solving $0 = \nabla_x \mathcal{L}_{\sigma_k}(x, z, \hat{x}_k, \hat{y}_k)$, which can be rewritten as the linear system

$$[\mu_k Q + \rho_k \mathbb{I} + A^\top A] x = (\rho_k \hat{x}_k - \mu_k q + A^\top(z - \hat{y}_k)). \quad (12)$$

Note that the matrix on the left-hand side is always symmetric positive definite, hence nonsingular, and independent on z , whereas the right-hand side vector varies linearly in z . Thus, \mathcal{X}_k is a linear map from \mathcal{C} to \mathbb{R}^n . Moreover, factorization caching can be adopted, effectively factorizing (at most) once for each solve of (CAL_k) . To avoid the matrix fill-in due to $A^\top A$, in our implementation we do not solve [\(12\)](#) as is, but lift it to recover structure; see [Section 4.2](#) below for details.

Given z , one can find the optimal $\mathcal{X}_k(z)$ and then evaluate $\mathcal{M}_k(z)$ directly through its definition [\(11\)](#). Owing to the chain rule, the gradient $\nabla \mathcal{M}_k(z)$ is readily obtained as

$$\nabla \mathcal{M}_k(z) = \nabla_z \mathcal{L}_{\sigma_k}(\mathcal{X}_k(z), z, \hat{x}_k, \hat{y}_k) = z - A \mathcal{X}_k(z) - \hat{y}_k,$$

since $\nabla_x \mathcal{L}_{\sigma_k}(\mathcal{X}_k(z), z, \hat{x}_k, \hat{y}_k) = 0$ by definition of \mathcal{X}_k .

4.2 Lower-level equality constraints

The formulation (1) offers a compact yet generic model to analyse. However, practical optimization models often exhibit a richer structure: linear dynamics in optimal control tasks give rise to linear equality constraints, say $A_{\text{eq}}x = b_{\text{eq}}$, that are “safe”, in the sense that they are feasible and non-redundant. Here we proceed to demonstrate how this additional structure can be exploited for speeding up Step 1 even further.

By keeping the equality constraints $A_{\text{eq}}x = b_{\text{eq}}$ without relaxation, we treat them as lower-level constraints in the AL subproblem (on par with the inclusion $z \in \mathcal{C}$) instead of including them in the augmented Lagrangian. Then, the counterpart of (10) is an equality-constrained quadratic program,

$$\mathcal{X}_k(z) := \arg \min_x \{\mathcal{L}_{\sigma_k}(x, z, \hat{x}_k, \hat{y}_k) \mid A_{\text{eq}}x = b_{\text{eq}}\},$$

whose solution requires only a linear system. Upon lifting with auxiliary variables λ and λ_{eq} , we write it as

$$\begin{bmatrix} \mu_k Q + \rho_k \mathbb{I} & A^\top & A_{\text{eq}}^\top \\ A & -\mathbb{I} & 0 \\ A_{\text{eq}} & 0 & 0 \end{bmatrix} \begin{pmatrix} x \\ \lambda \\ \lambda_{\text{eq}} \end{pmatrix} = \begin{pmatrix} \rho_k \hat{x}_k - \mu_k q - A^\top \hat{y}_k \\ z \\ b_{\text{eq}} \end{pmatrix}$$

to retain sparsity and symmetry; see [Section A.1](#) for details.

5 Numerical Results

We consider three different benchmarks: an initial value problem of a discontinuous dynamic with single switch, a discretized obstacle problem, and a reference tracking task with the AFTI-16 aircraft model.

We assess various solver configurations along two axes:

- subproblem: *extended* formulation (as in [\[8\]](#)) against the proposed *condensed* one (using the marginalization of [Section 4.1](#)). In the latter case, explicit equality constraints $A_{\text{eq}}x = b_{\text{eq}}$ are treated either as *soft* (relaxing them like $Ax = z$) or *hard* (according to [Section 4.2](#)).
- subsolver: NMPC (with spectral stepsize) [\[4\]](#) or PANOC⁺ (with quasi-Newton extrapolation) [\[5\]](#), both with nonmonotone linesearch.

Overall, six solver configurations are compared, with subproblem formulations that increasingly exploit the problem’s structure.

Solver setup Our prototypical implementation in MATLAB 2025a run on a standard laptop, Intel Core i7 2.80 GHz, 16 GB RAM. For each call to [Algorithm 3.1](#), we set a time limit of 100 s, tolerances $\epsilon_d = \epsilon_p = 10^{-6}$, and parameters $\kappa_\rho = 1$, $\rho_1 = 10^{-6}$, $\kappa_\mu = 1/4$, $\mu_1 = 1$, $\kappa_\varepsilon = 1/2$, $\varepsilon_1 = 1$, $\kappa_V = 9/10$, $Y := [-10^{20}, 10^{20}]^m$. For each problem instance, we consider 10 random (normally distributed) initializations for x^0 , and then set $y^0 = 0$, $z^0 = \text{proj}_{\mathcal{C}}(Ax^0)$.

Profiles Solvers are compared by means of data and (extended) performance profiles. For P the set of problem instances and S the set of solver settings, let $t_{s,p}$ denote the wall-clock runtime required by $s \in S$ on $p \in P$. When solver s fails on problem p , we set $t_{s,p} = \infty$. A *data profile* depicts the empirical distribution $f_s^{\text{abs}}: [0, \infty) \rightarrow [0, 1]$ of $t_{s,.}$ over P , namely $f_s^{\text{abs}}(t) := |\{p \in P \mid t_{s,p} \leq t\}|/|P|$, where $|P|$ denotes the cardinality of P . As such, each data profile reports the fraction of problems $f_s^{\text{abs}}(t)$ that can be solved (for given tolerances) by solver s with a computational budget t , and therefore it is independent of the other solvers. In contrast, an *extended performance profile* is relative to a pool of solvers S ; it depicts the empirical distribution $f_s^{\text{rel}}: [0, \infty) \rightarrow [0, 1]$ of the ratio $r_{s,.}$ of $t_{s,.}$ with the best runtime among the other solvers, namely $r_{s,p} := t_{s,p} / \min\{t_{s',p} \mid s' \in S, s' \neq s\}$, see [\[11, §4.1\]](#). A scalability analysis is provided in [Section A.4](#).

5.1 Initial value problem

Introduced by Stewart and Anitescu [16, §2], this test example contains a dynamical system with a discontinuous right-hand side, in which a single switch occurs. The discontinuous dynamics can be reformulated into a linear complementarity system. We then discretize the system using the implicit Euler scheme with N nodes, as in [6, §5.2], obtaining

$$\begin{aligned} & \underset{\substack{x_0, \dots, x_N \in \mathbb{R} \\ y_1, \dots, y_N \in \mathbb{R} \\ \lambda_1, \dots, \lambda_N \in \mathbb{R}}}{\text{minimize}} \quad (x_N - x_{\text{ref}})^2 + h \sum_{k=0}^{N-1} x_k^2 \\ & \text{subject to} \quad x_k = x_{k-1} + h(3 - 2y_k), \\ & \quad 0 \leq x_k + \lambda_k \perp 1 - y_k \geq 0, \\ & \quad 0 \leq \lambda_k \perp y_k \geq 0 \quad \text{for } k = 1, \dots, N \end{aligned} \tag{13}$$

with reference $x_{\text{ref}} := 5/3$ and time step $h = 2/N$.

Results with increasing number of discretization intervals $N \in \{2^3, 2^4, \dots, 2^8\}$, for a total of 60 calls to each solver, are reported in Figure 1. All profiles indicate that the *condensed* formulation beats the extended, with the *hard* treatment of equality constraints delivering better runtimes. For fixed subproblem, PANOC⁺ typically outperforms NMPG as subsolver. Moreover, we point out that, despite the generic approach powering Algorithm 3.1, it achieves performance on par with the solver developed in [6] specifically for complementarity constraints.

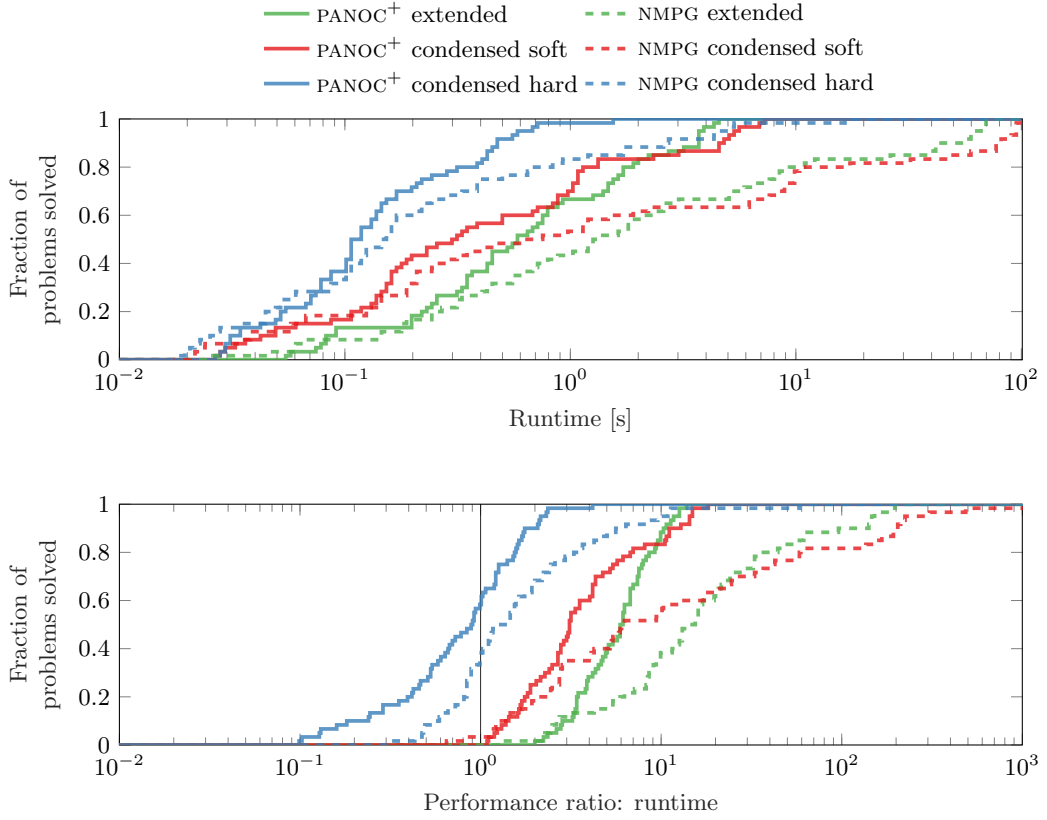


Figure 1: Initial value problem (13): data (top) and performance (bottom) profiles for comparing different solver settings.

5.2 Obstacle problem

We consider the optimal control of a discretized obstacle problem as investigated in [8, Example 6.2]. The problem is given by

$$\begin{aligned} & \underset{x, y, z \in \mathbb{R}^N}{\text{minimize}} \quad \frac{1}{2} \|x\|^2 + \frac{1}{2} \|y\|^2 - \langle 1, y \rangle \\ & \text{subject to} \quad x \geq 0, \quad \min\{y, z\} = 0, \quad x + Ay = z \end{aligned} \quad (14)$$

where $A \in \mathbb{R}^{N \times N}$ is a tridiagonal matrix that arises from a discretization of the negative Laplace operator in one dimension. Its simple solution $x = y = z = 0$ is degenerate and makes the problem particularly arduous to solve.

The numerical results depicted in Figure 2 lead to observations analogous to those for Figure 1. Compared to [8, §6.1], we can push the discretization from their $N = 64$ to $N = 256$ and, using PANOC⁺ as subsolver, keep a reasonable runtime and the total number of inner iterations in the order of thousands instead of millions.

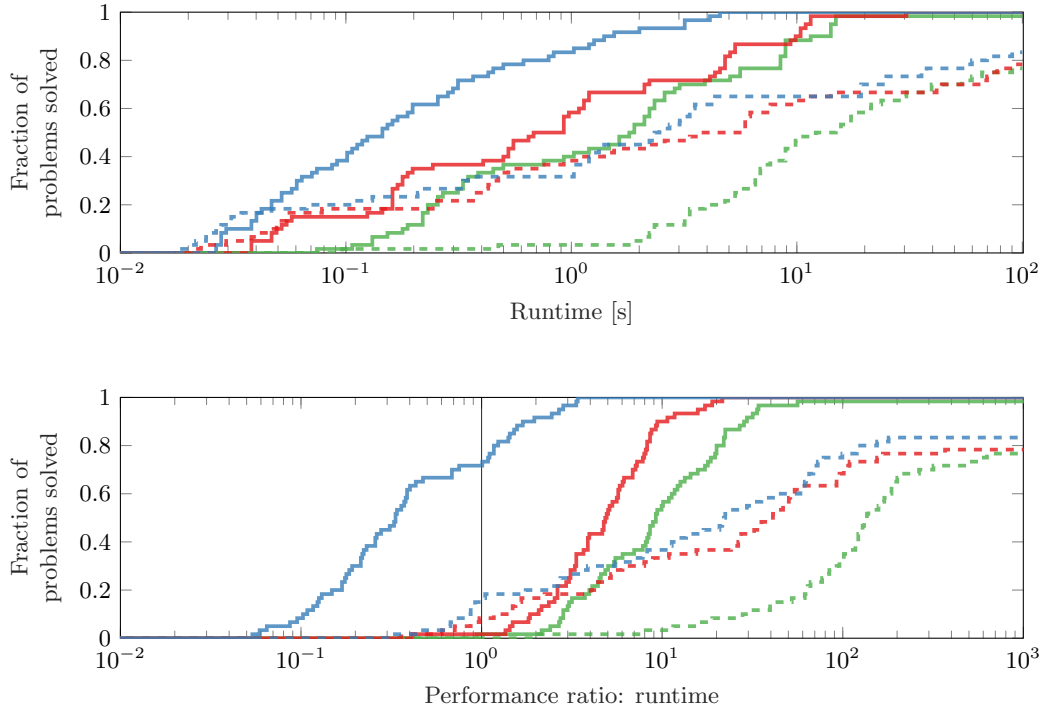


Figure 2: Obstacle problem (14): data (top) and performance (bottom) profiles for comparing different solver settings. Legend as in Figure 1.

5.3 AFTI-16 tracking control

The AFTI-16 model from [10] provides a LTI approximation of the aircraft's longitudinal dynamics at 3000 ft altitude and 0.6 Mach speed: the state description includes forward velocity, angle of attack, pitch rate, and pitch angle, while control inputs are elevator and flaperon angles. The model, converted to discrete time by sampling with zero-order hold on the inputs and a sample time of $T_s = 50$ ms, is

$x_{k+1} = A_{\text{DT}}x_k + B_{\text{DT}}u_k$ with

$$A_{\text{DT}} = \begin{bmatrix} 0.9993 & -3.0083 & -0.1131 & -1.6081 \\ -4.703 \cdot 10^{-6} & 0.9862 & 0.0478 & 3.85 \cdot 10^{-6} \\ 3.703 \cdot 10^{-6} & 2.0833 & 1.0089 & -4.362 \cdot 10^{-6} \\ 1.356 \cdot 10^{-7} & 0.0526 & 0.0498 & 1 \end{bmatrix}$$

$$B_{\text{DT}} = \begin{bmatrix} -0.08045 & -0.6347 \\ -0.02914 & -0.01428 \\ -0.8679 & -0.0913 \\ -0.02159 & -0.002181 \end{bmatrix}, \quad C_{\text{DT}}^\top = \begin{bmatrix} 0 & 0 \\ 1 & 0 \\ 0 & 0 \\ 0 & 1 \end{bmatrix};$$

more details in [Section A.3](#). The control task is to track the null reference for the observed states, with an additional cost for the control effort:

$$\begin{aligned} & \underset{\substack{x_1, \dots, x_N \in \mathbb{R} \\ u_0, \dots, u_{N-1} \in \mathbb{R}}}{\text{minimize}} \quad \sum_{k=0}^{N-1} \|C_{\text{DT}}x_{k+1}\|^2 + \left\| \frac{u_k}{u_{\max}} \right\|^2 \\ & \text{subject to} \quad x_{k+1} = A_{\text{DT}}x_k + B_{\text{DT}}u_k, \\ & \quad u_k \in U \quad \text{for } k = 0, \dots, N-1. \end{aligned} \quad (15)$$

The initial state $x_0 = x_{\text{init}}$ is fixed, as well as the time horizon N . As detailed in (15), the control system is also subject to a geometric constraint on the admissible controls. Set $U := \{(a, b) \in \mathbb{R}^2 \mid |a| \leq u_{\max}, |b| \leq u_{\max}, ab = 0\}$ encodes an either-or condition intersected with simple bounds: at any given time, at most one control input can be applied, and its magnitude cannot be larger than $u_{\max} := 25$.

The outcomes depicted in [Figure 3](#) (obtained with randomized x_{init}) demonstrate an even greater advantage for the condensed formulation with hard equality constraints. Moreover, compared to previous examples, the performance in this case seems less dependent on the subsolver.

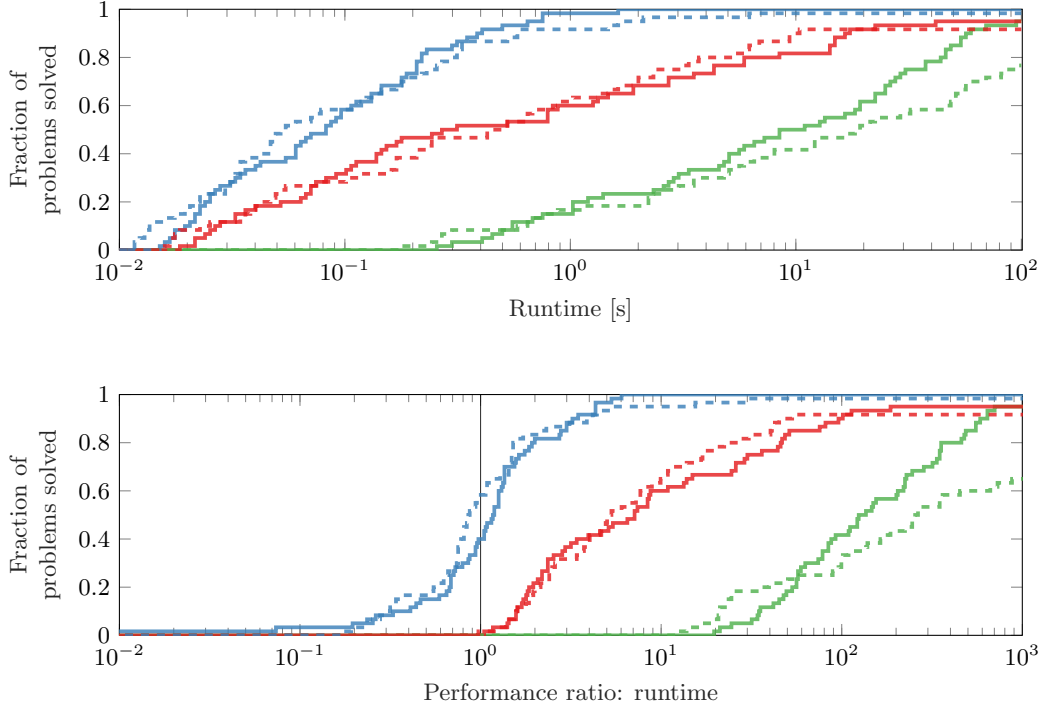


Figure 3: AFTI-16 problem (13): data (top) and performance (bottom) profiles for comparing different solver settings. Legend as in [Figure 1](#).

To assess the quality of solutions, we repeatedly solve (15) in a simulated environment with closed-loop control; here we start from $x_0 = (10, 10, 10, 10)$ and use the solver configuration “NMPG condensed

hard”. Numerical results with and without warm-starting the solver are reported in Figure 4. Despite the nonconvex admissible set U , the solver quickly finds sufficiently good control sequences to steer the system as desired, also counteracting the disturbance injected at $t = 2.5$.

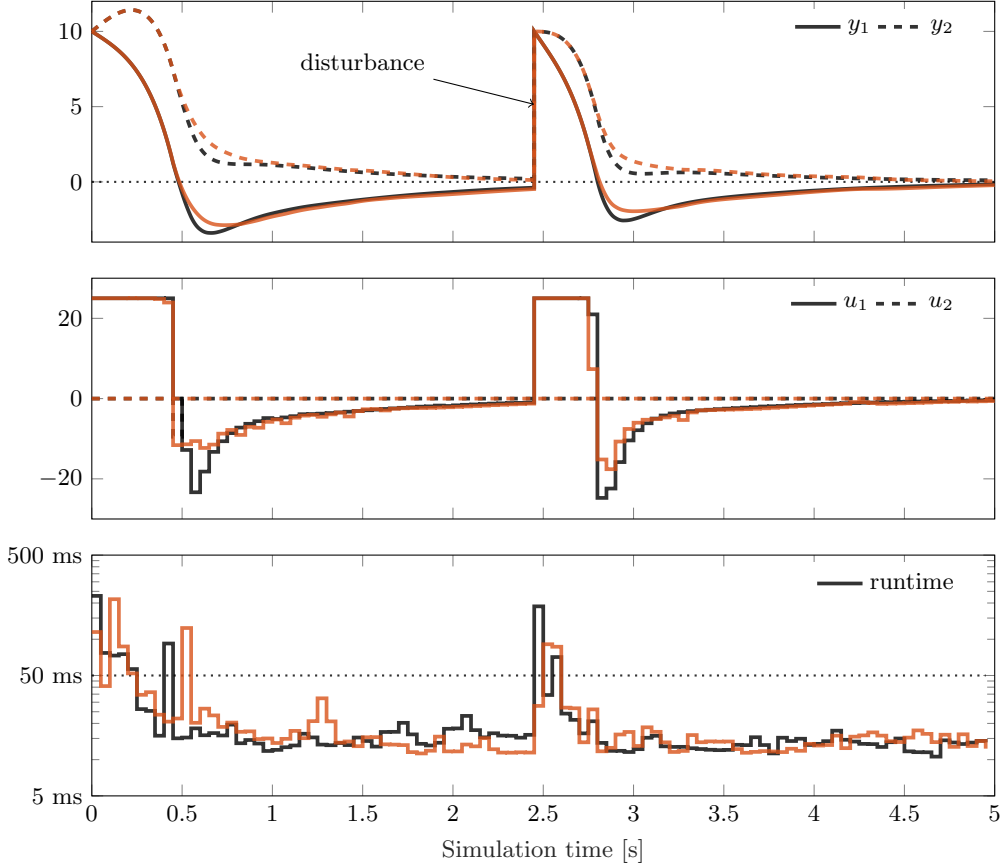


Figure 4: Closed-loop simulation of AFTI-16 behavior: outputs (top), inputs (middle) and solver runtime (bottom) using cold- (black) or warm-starting (orange) between consecutive simulation steps. A disturbance is injected at half time, resetting the observed states as at the initial time.

6 Conclusions

In this article, we introduced a structure-exploiting approach for addressing linear-quadratic optimization problems with geometric constraints. Our strategy inherits convergence guarantees from the augmented Lagrangian framework and builds upon simple and efficient computational kernels. Making analytical progress in the subproblem formulation, we effectively precondition it and reduce its size to advantage of the user-defined subsolver. Extensive numerical experiments demonstrate significant speed-up and improved robustness.

References

- [1] P. Armand and N. N. Tran. An augmented Lagrangian method for equality constrained optimization with rapid infeasibility detection capabilities. *Journal of Optimization Theory and Applications*, 181(1):197–215, 2019. doi:[10.1007/s10957-018-1401-7](https://doi.org/10.1007/s10957-018-1401-7).
- [2] E. G. Birgin and J. M. Martínez. *Practical Augmented Lagrangian Methods for Constrained Optimization*. Society for Industrial and Applied Mathematics, Philadelphia, PA, 2014. doi:[10.1137/1.9781611973365](https://doi.org/10.1137/1.9781611973365).

- [3] S. Cafieri, A. R. Conn, and M. Mongeau. Mixed-integer nonlinear and continuous optimization formulations for aircraft conflict avoidance via heading and speed deviations. *European Journal of Operational Research*, 310(2):670–679, 2023. doi:[10.1016/j.ejor.2023.03.002](https://doi.org/10.1016/j.ejor.2023.03.002).
- [4] A. De Marchi. Proximal gradient methods beyond monotony. *Journal of Nonsmooth Analysis and Optimization*, 4, 2023. doi:[10.46298/jnsao-2023-10290](https://doi.org/10.46298/jnsao-2023-10290).
- [5] A. De Marchi and A. Themelis. Proximal gradient algorithms under local Lipschitz gradient continuity. *Journal of Optimization Theory and Applications*, 194(3):771–794, 2022. doi:[10.1007/s10957-022-02048-5](https://doi.org/10.1007/s10957-022-02048-5).
- [6] J. Hall, A. Nurkanović, F. Messerer, and M. Diehl. LCQPow: a solver for linear complementarity quadratic programs. *Mathematical Programming Computation*, 17(1):81–109, 2025. doi:[10.1007/s12532-024-00272-w](https://doi.org/10.1007/s12532-024-00272-w).
- [7] T. Hoheisel, C. Kanzow, and A. Schwartz. Mathematical programs with vanishing constraints: a new regularization approach with strong convergence properties. *Optimization*, 61(6):619–636, 2012. doi:[10.1080/02331934.2011.608164](https://doi.org/10.1080/02331934.2011.608164).
- [8] X. Jia, C. Kanzow, P. Mehlitz, and G. Wachsmuth. An augmented Lagrangian method for optimization problems with structured geometric constraints. *Mathematical Programming*, 199(1):1365–1415, 2023. doi:[10.1007/s10107-022-01870-z](https://doi.org/10.1007/s10107-022-01870-z).
- [9] C. Kanzow, P. Mehlitz, and D. Steck. Relaxation schemes for mathematical programmes with switching constraints. *Optimization Methods and Software*, pages 1–36, 2019. doi:[10.1080/10556788.2019.1663425](https://doi.org/10.1080/10556788.2019.1663425).
- [10] P. Kapasouris, M. Athans, and G. Stein. Design of feedback control systems for unstable plants with saturating actuators. In *Proc. IFAC Symposium on Nonlinear Control System Design*, pages 302–307. Pergamon Press, 1990.
- [11] A. Mahajan, S. Leyffer, and C. Kirches. Solving mixed-integer nonlinear programs by QP-diving. Anl/mcs preprint p2071-0312, Argonne National Laboratory, 2012.
- [12] E. Ménager, A. Bambade, W. Jallet, A. De Marchi, and J. Carpentier. Contact-implicit inverse dynamics. *IEEE Transactions on Robotics*, 2025, [hal-05201780](https://hal.archives-ouvertes.fr/hal-05201780). under review.
- [13] V. Nikitina, A. De Marchi, and M. Gerdts. Hybrid optimal control with mixed-integer Lagrangian methods. *IFAC-PapersOnLine*, 2025, [2403.06842](https://doi.org/10.1080/2403.06842). 13th IFAC Symposium on Nonlinear Control Systems (NOLCOS).
- [14] K. Palagachev and M. Gerdts. Mathematical programs with blocks of vanishing constraints arising in discretized mixed-integer optimal control problems. *Set-Valued and Variational Analysis*, 23(1):149–167, 2015. doi:[10.1007/s11228-014-0297-0](https://doi.org/10.1007/s11228-014-0297-0).
- [15] N. Robuschi, C. Zeile, S. Sager, and F. Braghin. Multiphase mixed-integer nonlinear optimal control of hybrid electric vehicles. *Automatica*, 123:109325, 2021. doi:[10.1016/j.automatica.2020.109325](https://doi.org/10.1016/j.automatica.2020.109325).
- [16] D. E. Stewart and M. Anitescu. Optimal control of systems with discontinuous differential equations. *Numerische Mathematik*, 114(4):653–695, 2010. doi:[10.1007/s00211-009-0262-2](https://doi.org/10.1007/s00211-009-0262-2).
- [17] P. Zheng, T. Askham, S. L. Brunton, J. N. Kutz, and A. Y. Aravkin. A unified framework for sparse relaxed regularized regression: SR3. *IEEE Access*, 7:1404–1423, 2019. doi:[10.1109/ACCESS.2018.2886528](https://doi.org/10.1109/ACCESS.2018.2886528).

A Additional Material

A.1 Globally Lipschitz gradient

Let us denote $\|\mathcal{X}_k\|$ the operator norm of \mathcal{X}_k , which depends on the problem data as well as on parameters σ_k . Now we proceed to show that, for each $k \in \mathbb{N}$, \mathcal{M}_k has globally Lipschitz continuous gradient, regardless of the problem data and choice of parameters σ_k . Picking two arbitrary $z_1, z_2 \in \mathbb{R}^m$ and invoking the triangle and Cauchy-Schwartz inequalities, we have the bound

$$\begin{aligned}\|\nabla \mathcal{M}_k(z_1) - \nabla \mathcal{M}_k(z_2)\| &= \|\nabla_z \mathcal{L}_{\sigma_k}(\mathcal{X}_k(z_1), z_1, \hat{x}_k, \hat{y}_k) - \nabla_z \mathcal{L}_{\sigma_k}(\mathcal{X}_k(z_2), z_2, \hat{x}_k, \hat{y}_k)\| \\ &= \|(z_1 - A\mathcal{X}_k(z_1) - \hat{y}_k) - (z_2 - A\mathcal{X}_k(z_2) - \hat{y}_k)\| \\ &= \|A[\mathcal{X}_k(z_2) - \mathcal{X}_k(z_1)] + (z_1 - z_2)\| \\ &\leq \|A[\mathcal{X}_k(z_2) - \mathcal{X}_k(z_1)]\| + \|z_1 - z_2\| \\ &\leq \|A\|\|\mathcal{X}_k(z_2) - \mathcal{X}_k(z_1)\| + \|z_1 - z_2\| \\ &\leq (\|A\|\|\mathcal{X}_k\| + 1)\|z_1 - z_2\|.\end{aligned}$$

Since \mathcal{X}_k is a linear operator (also in the presence of equalities $A_{\text{eq}}x = b_{\text{eq}}$), the finite quantity $L_{\mathcal{M}_k} := \|A\|\|\mathcal{X}_k\| + 1$ represents a global Lipschitz constant for $\nabla \mathcal{M}_k$.

A.2 Structured linear system

Let us derive step-by-step the linear system in [Section 4.2](#). Given some $z \in \mathcal{C}$, the optimal $x = \mathcal{X}_k(z)$ is obtained as the unique solution to

$$\begin{aligned}\underset{x}{\text{minimize}} \quad & \mu_k f(x) + \frac{1}{2} \|Ax - z + \hat{y}_k\|^2 + \frac{\rho_k}{2} \|x - \hat{x}_k\|^2 \\ \text{subject to} \quad & A_{\text{eq}}x = b_{\text{eq}}.\end{aligned}$$

The optimality conditions for this problem read

$$\begin{aligned}0 &= \mu_k(Qx + q) + A^\top(Ax - z + \hat{y}_k) + A_{\text{eq}}^\top \lambda_{\text{eq}} + \rho_k(x - \hat{x}_k) \\ 0 &= A_{\text{eq}}x - b_{\text{eq}}\end{aligned}$$

where λ_{eq} denotes the Lagrange multiplier for $A_{\text{eq}}x = b_{\text{eq}}$. Introducing the auxiliary variable $\lambda \equiv Ax - z$, we can write the equivalent system of linear equations

$$\begin{aligned}0 &= \mu_k(Qx + q) + A^\top(\lambda + \hat{y}_k) + A_{\text{eq}}^\top \lambda_{\text{eq}} + \rho_k(x - \hat{x}_k) \\ 0 &= Ax - z - \lambda \\ 0 &= A_{\text{eq}}x - b_{\text{eq}},\end{aligned}$$

which can be rearranged in matrix form obtaining the one in [Section 4.2](#).

A.3 AFTI-16 model

The continuous-time (dynamics and observation) model from [\[10\]](#) is $\dot{x} = A_{\text{CT}}x + B_{\text{CT}}u$, $y = C_{\text{CT}}x$ with

$$\begin{aligned}A_{\text{CT}} &= \begin{bmatrix} -0.0151 & -60.5651 & 0 & -32.174 \\ -0.0001 & -1.3411 & 0.9929 & 0 \\ 0.00018 & 43.2541 & -0.86939 & 0 \\ 0 & 0 & 1 & 0 \end{bmatrix} \\ B_{\text{CT}} &= \begin{bmatrix} -2.516 & -13.136 \\ -0.1689 & -0.2514 \\ -17.251 & -1.5766 \\ 0 & 0 \end{bmatrix}, \quad C_{\text{CT}}^\top = \begin{bmatrix} 0 & 0 \\ 1 & 0 \\ 0 & 0 \\ 0 & 1 \end{bmatrix}.\end{aligned}$$

The discrete-time counterpart given in [Section 5.3](#) was obtained with MATLAB's Control System Toolbox via the commands

```

>> plantCT = ss(A_CT, B_CT, C_CT, D_CT);
>> plantDT = c2d(plantCT, Ts);

```

and taking the state-space matrix representation of `plantDT` with four decimals for each entry. Both models have $D_{CT} = D_{DT} = 0$ and $C_{CT} = C_{DT} \neq 0$.

A.4 Scalability outcomes

In addition to the data and performance profiles presented in Section 5, we report here *scalability profiles*. These display the median values and the interquartile range over all instances of a given size, indicating how the metric is affected by the problem size.

Scalability profiles are depicted in Figure 5. It appears that, among all solver configurations, the condensed, hard formulation with PANOC⁺ subsolver consistently performs best and scales better with problem size. The solver settings with PANOC⁺ are significantly more effective than with NMPG for problems (13) and (14), but they are surprisingly similar for (15).

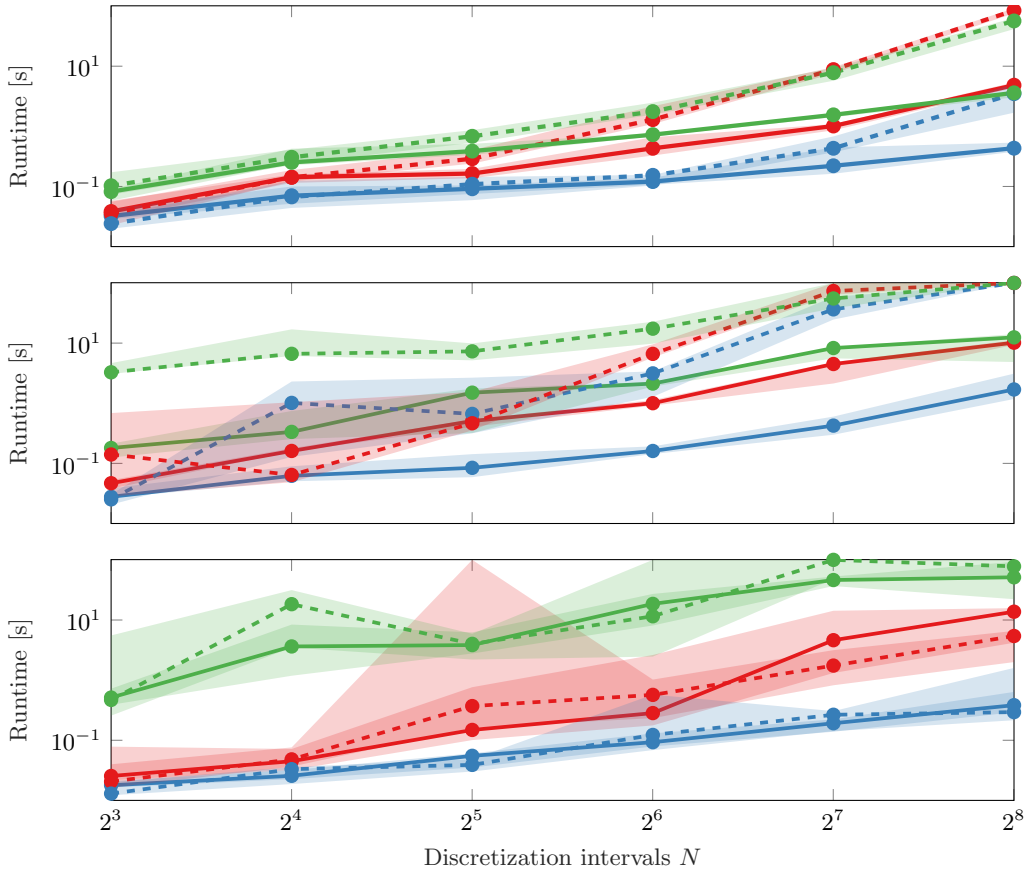


Figure 5: Scalability profiles for comparing different solver settings: initial value problem (13) (top), obstacle problem (14) (middle) and AFTI-16 problem (15) (bottom). Legend as in Figure 1.